Predictive Quantization and Joint Time-Frequency interpolation technique for MIMO-OFDM precoding

Agrim Gupta*, Kumar Appaiah*, Rahul Vaze†
*Department of Electrical Engineering, Indian Institute of Technology Bombay
† School of Technology and Computer Science, Tata Institute of Fundamental Research

***Abstract*—Precoding transmissions in wireless MIMO systems is essential to enable optimal utilization of the spatial degrees of freedom. However, communicating the precoding matrices from the receiver is challenging, owing to large feedback requirements. Past work has shown that predictive quantization in time, as well as interpolation over frequency can be used to reconstruct the precoders over a wide band, although these techniques have not been used jointly. We propose both a predictive quantization as well as a joint time-frequency interpolation strategy for precoding matrices over the Stiefel manifold. The key insight that we use is that local tangent spaces in the manifold permit effective combination of both temporal and frequency domain information for more accurate precoder reconstruction. Simulations reveal that we obtain a significant improvement in achievable rate as well as BER reduction when compared to existing strategies.**

I. Introduction

The use of orthogonal frequency division multiplexing (OFDM) in multi-antenna ($N_T \times N_R$) wireless systems allows the treatment of a frequency-selective channel as a frequency-flat multiple-input multiple-output (MIMO) channel on a per subcarrier basis. This enables low-complexity receiver implementations, particularly for equalization. To maximally utilize the benefit, the receiver needs to feedback channel state information (CSI) to the transmitter, which then uses it for precoding (matrix transformation of the input signal) to accomplish waterfilling or for efficient signaling to increase rate while reducing bit-error-rate (BER) [1].

Modern wireless OFDM systems support thousands of subcarriers, thus the CSI requirement is rather large, however, only a limited number of bits are reserved for CSI transmission. This necessitates exploiting the underlying manifold structure of the channel/precoding matrices for quantization and interpolation [2] across frequencies and time. Utilizing the frequency/ temporal correlation to improve channel estimates has been considered in [3–8]. The manifold structure permits reconstruction and prediction of precoders at unknown locations.

Typical approaches for quantization over manifolds involves unitary manifolds, where the quantization is implemented over the full $N_T \times N_T$ unitary space. When $N_T > N_R$, the effective dimensions are given by $N_T \times N_R$ matrices residing in the Stiefel manifold. Stiefel manifolds can be used to work with the effective dimensions, thereby reducing the CSI overhead, however, computing geodesics (shortest paths) over the Stiefel manifolds is challenging. In recent work, a Lloyd type codebook scheme has been suggested for direct quantization of matrices residing in Stiefel manifold [9] and it has been shown that closed form unique quasi-geodesics can be computed over Stiefel manifold [10]. We exploit both of these recent results to reduce the overhead requirement by quantizing at the receiver and interpolating at the transmitter, both while working with the effective dimensions of the Stiefel manifold.

In addition to working over the reduced space using the Stiefel manifold quasi-geodesics, we also focus on jointly exploiting the temporal and frequency correlation for efficient limited CSI feedback. To the best of our knowledge, prior work has considered quantization over the Stiefel manifold only in the presence temporal correlation [11] or in frequency domain [12] but not jointly. Exploiting temporal and frequency correlation presents novel challenges, and we propose a predictive quantization and interpolation strategy which exploits the temporal and frequency correlations jointly over the Stiefel manifold, building upon the ideas presented in [4, 11].

We provide extensive simulations to illustrate the benefits of our approach in terms of improving the BER, the achievable rate and channel estimation error (measured via the chordal distance). Our approach outperforms the best known strategies in the literature by about 2 dB in terms of BER, and significant improvement in terms of sum-rate for the same number of feedback bits. The chordal distance also reduces by over 50%.

II. System Model

We consider a point-to-point MIMO-OFDM wireless system that has N_T transmit antennas and N_R receive antennas. The available bandwidth is divided into N subcarriers such that each subcarrier has a nearly flat frequency response, as is commonly the case in the OFDM systems. The transmitter communicates an $N_s \times 1$ data vector, where $N_s \leq \min(N_T, N_R)$, and the $N_T \times N_s$ precoding matrix maps the $N_s \times 1$ data vector onto the $N_T \times 1$ transmit vector emanating out of the transmitter. In this discussion, we assume that $N_T > N_R$ and $N_s = N_R$. Keeping notations consistent with [11], the $N_R \times 1$ data stream received is denoted by

$$\mathbf{y}_{i,t} = \mathbf{H}_{i,t}^H \tilde{\mathbf{U}}_{i,t} \mathbf{x}_{i,t} + \mathbf{w}_{i,t} \tag{1}$$

where $\tilde{\mathbf{U}}_{i,t} \in \mathbb{C}^{N_T \times N_R}$ denotes the precoding matrix which is a function of quantized channel information fed back by the receiver, $\mathbf{y}_{i,t} \in \mathbb{C}^{N_R \times 1}$ is the received data stream, $\mathbf{x}_{i,t} \in \mathbb{C}^{N_R \times 1}$

Parts of this work was supported by the Bharti Centre for Communication in IIT Bombay, and the Visvesvaraya PhD Scheme of Ministry of Electronics & Information Technology, Government of India (implemented by the Digital India Corporation).

denotes the transmitted signal at the i-th subcarrier of the t-th OFDM frame, $\mathbf{H}_{i,t} \in \mathbb{C}^{N_T \times N_R}$ denotes the MIMO channel matrix and $\mathbf{w}_{i,t}$ denotes the i.i.d. complex Gaussian noise with $\mathbf{w}_{i,t} \sim \mathcal{N}_{\mathbb{C}}(0, N_0 \mathbf{I}_{N_R})$, N_0 being the noise variance.

If the accurate channel matrices $\mathbf{H}_{i,t}^H$ are available at the transmitter, the optimal policy is to use the right singular vectors of $\mathbf{H}_{i,t}^H$ as the precoding matrices $\tilde{\mathbf{U}}_{i,t}$ to maximize the mutual information or the SNR. In particular, if SVD$(\mathbf{H}_{i,t}) = \mathbf{U}_{i,t}, \Sigma_{i,t}, \mathbf{V}_{i,t}$, then $\tilde{\mathbf{U}}_{i,t} = \mathbf{U}_{i,t}$. Notice that matrices $\mathbf{U}_{i,t}$ reside on the Stiefel manifold $\mathrm{St}(N_T, N_R)$, since the columns of $\mathbf{U}_{i,t}$ form a set of N_R orthogonal vectors in N_T dimensions. Given practical limitations, only limited feedback is available from the receiver, and the objective is to find 'reasonable' estimate of $\mathbf{U}_{i,t}$, given by $\tilde{\mathbf{U}}_{i,t}$ using the available feedback bits.

We consider the chordal distance metric on the Stiefel manifold that is defined as $d_s(\mathbf{A}, \mathbf{B}) = \sqrt{\sum_{j=1}^{N_R} d_g^2(\mathbf{a}_j, \mathbf{b}_j)}$, where $\mathbf{A}, \mathbf{B} \in \mathrm{St}\{N_T, N_R\}$, and $\mathbf{a}_j, \mathbf{b}_j$ is the j-th column of $\mathbf{A}$, $\mathbf{B}$ respectively, and $d_g(\mathbf{u}, \mathbf{v}) = \sqrt{1 - |\mathbf{u}^* \mathbf{v}|^2}$ is the Grassmannian chordal distance [5]. Thus, the objective is to obtain an estimate $\hat{\mathbf{U}}_{i,t}$ of $\mathbf{U}_{i,t}$ that minimizes the chordal distance between $\hat{\mathbf{U}}_{i,t}$ and $\mathbf{U}_{i,t}$ on the Stiefel manifold.

Frequency and time dependent channel matrices $\mathbf{H}_{i,t}^H$ (and consequently $\mathbf{U}_{i,t}$), pose an additional challenge with limited feedback, since feeding back $\mathbf{U}_{i,t}$ for each i and t is prohibitive. This makes exploiting of the frequency and temporal correlation structure imperative. Feeding back $\mathbf{U}_{i,t}$ at regular frequency and time intervals and employing a naïve linear interpolation does not work, since the precoding matrices do not form a vector space. Several approaches in literature exploit the underlying manifold structure but have largely exploited frequency or temporal correlation in isolation for interpolation and prediction [4, 6, 8, 11, 13, 14]. For the case where the precoding matrices reside on the Stiefel manifold, temporal correlation has been used in [11] and an interpolation algorithm has been suggested in [12]. A non-manifold based approach to simultaneously capture frequency and temporal correlation is presented in [15]. In this paper, we present a manifold based approach to estimate the precoding matrices under limited feedback that exploit both the frequency and temporal correlations. Our approach exploits the differential geometry of the Stiefel manifold. We assume that zero-delay limited feedback is available at the transmitter, and the channel matrix $\mathbf{H}_{i,t}^H$ is estimated perfectly at the receiver.

We represent the limited feedback setting by a time-frequency bin matrix (Fig. 1), where information about time-frequency bins is sparsely fed back by the receiver. The transmitter estimates the matrices at each non fed-back point by utilizing the temporal and frequency correlations. The metric we choose to compare two estimates of the time-frequency bin matrix is $d[t] = \frac{1}{N} \sum_{i=0}^{N-1} d_s(\tilde{\mathbf{U}}_{i,t}, \mathbf{U}_{i,t})$. Observe that $d[t_1]$ at a particular time t_1 represents the average chordal distance between the estimates and actual values of row t_1 in the time-frequency bins matrix. Using the prior work on predictive quantization over $\mathrm{St}(N_T, N_R)$ [11] along with the modifications suggested in Section III, one can fill the time-frequency bin matrix using the strategy shown in Fig. 1 by sending feedback on regularly spaced subcarrier indices. This strategy captures frequency and time correlations independently. A lower $d[t]$ may potentially be obtained over time by capturing the time and frequency correlations jointly, which leads to improved performance and is outlined in Section IV.

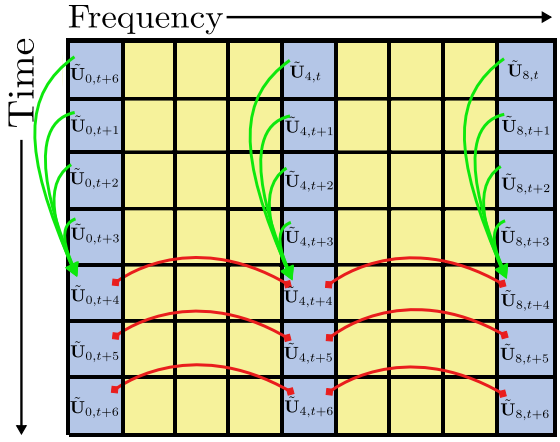

Fig. 1: Exploiting regularly spaced limited feedback scheme for $N = 9$, with (yellow) blue cells indicating the (non) fed back indices. Frequency correlations are captured via the red interpolating curves, and the temporal correlations are used to improve the quantization over time (shown implicitly via green arrows).

III. Proposed Interpolation on $St(N_T, N_R)$

In this section, we describe the interpolation scheme that allows interpolation along both the time and frequency (independently) domain over the Stiefel manifold. Doing this allows us to populate the time- frequency bins matrix with the strategy depicted in Fig. 1 and hence generalizes predictive quantization strategy in [11] for the MIMO-OFDM case.

Taking the full SVD of MIMO channel matrix $\mathbf{H}_{i,t}$ yields $\mathcal{U}_{i,t}, \Sigma_{i,t}, \mathbf{V}_{i,t}$, where $\mathcal{U}_{i,t} \in \mathbb{C}^{N_T \times N_T}$ is a unitary matrix, $\Sigma_{i,t} \in \mathbb{C}^{N_T \times N_R}$ is a diagonal matrix, and $\mathbf{V}_{i,t} \in \mathbb{C}^{N_R \times N_R}$ is a unitary matrix. Here, the optimal precoder consists of the first N_R columns of $\mathcal{U}_{i,t}$ [2]. $\tilde{\mathcal{U}}_{i,t}$ is the quantized value of $\mathcal{U}_{i,t}$. The usual approach using geodesic interpolation is as follows. Let us suppose that $\tilde{\mathcal{U}}_{i,t}$ have been fed back for subcarriers i_1 and i_2, $i_1 < i_2$. The transmitter interpolates via geodesic scheme [2] to obtain the $\tilde{\mathcal{U}}_{i,t}$ between i_1 and i_2 via

$$\tilde{\mathcal{U}}_{i,t} = \tilde{\mathcal{U}}_{i_1,t} \mathrm{expm}\left(\frac{i}{i_2 - i_1} \mathrm{logm}(\tilde{\mathcal{U}}_{i_1,t}^{-1} \tilde{\mathcal{U}}_{i_2,t}) \right) \tag{2}$$

where expm$(\cdot)$ and logm$(\cdot)$ refer to the matrix exponential and matrix logarithm, respectively. The precoding matrices are then obtained by taking the first N_R columns of the $\tilde{\mathcal{U}}_{i,t}$ matrices obtained after interpolation, since we require only the first N_R right singular vectors. The remaining $N_T - N_R$ ones, which were included in the setting to form the unitary matrix and enable interpolation with geodesics are actually redundant.

We now propose a method to directly interpolate over the Stiefel manifold, thereby obviating the need to quantize the redundant information. A natural approach would be to use geodesics, but true geodesic curves with closed form solution in the Stiefel manifold are not known [16]. Recently, [10]

has proposed a unique quasi geodesic curve using the Cayley type lifting-retraction maps that enable direct interpolation on $\mathrm{St}(N_T, N_R)$. Interpolation directly on $\mathrm{St}(N_T, N_R)$ has been discussed only in [12], albeit for unquantized precoders.

Let us suppose that $\tilde{\mathbf{U}}_{i,t}$ have been fed back for subcarriers i_1 and i_2, $i_1 < i_2$. We propose an interpolation method to obtain $\tilde{\mathbf{U}}_{i,t}$, similar to the geodesic interpolation in Equation 2 using the Cayley exponential lifting and retraction maps at $\tilde{\mathbf{U}}_{i_i,t}$, denoted as $\mathrm{Exp}^{-1}_{\tilde{\mathbf{U}}_{i_1,t}}(\cdot)$ and $\mathrm{Exp}_{\tilde{\mathbf{U}}_{i_1,t}}(\cdot)$ respectively, consistent with the notation in [10]. The transmitter interpolates via the below equation to obtain the $\tilde{\mathbf{U}}_{i,t}$ between i_1 and i_2

$$\tilde{\mathbf{U}}_{i,t} = \mathrm{Exp}_{\tilde{\mathbf{U}}_{i_1,t}}\left(\mathrm{Exp}^{-1}_{\tilde{\mathbf{U}}_{i_1,t}}\left(\tilde{\mathbf{U}}_{i_2,t}\right)\right) \tag{3}$$

One thing to note is that the $\mathrm{logm}(\cdot)$ maps $N_T \times N_T$ unitary matrices to $N_T \times N_T$ skew-Hermitian matrices. Similarly, the $\mathrm{Exp}^{-1}(\cdot)$ in Equation 3 maps $N_T \times N_R$ matrices on $\mathrm{St}(N_T, N_R)$ to $N_T \times N_T$ skew-Hermitian matrices, with the lower right $(N_T - N_R) \times (N_T - N_R)$ minor being the null matrix. A more detailed treatment is available in [10].

By using the approach described in (3) the receiver needs to quantize and feed back only $N_T \times N_R$ matrices $\mathbf{U}_{i,t}$, with $\mathbf{U}^H_{i,t}\mathbf{U}_{i,t} = \mathbf{I}_{N_R}$ instead of $N_T \times N_T$ unitary matrices $\mathcal{U}_{i,t}$, thereby obviating the need to quantize redundant information. The results, codebook generation and other nuances for the simulations for these approaches are described in Section V.

IV. Predictive Quantization and Joint Time-Frequency Interpolation

In this section, we describe a predictive quantization method employed by the receiver, coupled with an interpolation scheme at the transmitter to exploit both temporal and frequency correlations to enable more efficient reconstruction of the time-frequency bins matrix with a lower $d[t]$ metric and improved performance (BER and achievable rate).

A. Hopping and Predictive Quantization scheme

The approach for interpolation and prediction shown in Figure 1 is limited, in that the channel is fed back only at a fixed set of subcarriers, and the remaining subcarriers' precoders are interpolated. This method has two disadvantages. One is that the precoders for those subcarriers that lie in the middle of the subcarriers whose precoders have been fed back, face larger interpolation errors, since they are equally far away from the subcarriers where feedback is available. The other is that, while predictively quantizing over the time-domain, we ignore the useful past information present in the nearby subcarriers due to frequency correlations. We, therefore, suggest a "hopping" scheme, in which the fed back frequency bins are alternated in time. Let D_f be the frequency separation between two precoders estimated at the receiver, and δ_f be the frequency offset of the hopping scheme, both measured in terms of number of subcarriers (depicted in Fig. 2). We choose D_f as a factor of $N-1$, where N is the total number of subcarriers. We alternate between feeding back the precoder at subcarriers $\{mD_f | m = 0, 1, 2, \ldots (N-1)/D_f\}$ in one OFDM frame and subcarriers $\{\delta_f + mD_f | m = 0, 1, 2, \ldots (N-1)/D_f - 1\}$ in the next. We set $\delta_f = \lfloor D_f/2 \rfloor$ to address the issue of large interpolation errors in the middle of two fed back precoders. This permits us to obtain a more accurate reconstruction of the precoder variation across frequency, enabling more effective predictive quantization.

In the subsequent discussions, we refer to the value of the precoding matrix at subcarrier i at time t, $\tilde{\mathbf{U}}_{i,t}$, merely by referring to it as the precoder at box (i,t). Consider the hopping scheme described in Fig. 2. The yellow boxes indicate the time-frequency bins for which the quantized $\tilde{\mathbf{U}}_{i,t} \in \mathrm{St}\{N_T, N_R\}$ were fed back. The white boxes indicate the time-frequency bins where the precoding matrices that were not fed back.

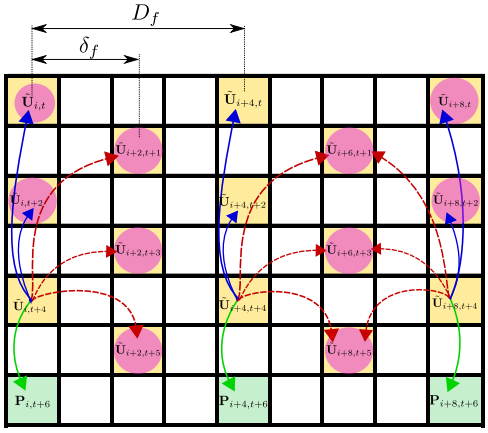

Fig. 2: Hopping strategy for $N = 9$, $D_f = 4$, $\delta_f = 2$. The red, blue and green curves represent the tangents on $\mathrm{St}(N_T, N_R)$, illustrated in Fig. 3.

For the t-th OFDM frame, the transmitter uses the past fed back information to obtain a prediction for those boxes where the receiver would provide feedback. This situation is depicted in Fig. 2 for the $(t+6)$-th OFDM frame. The feedback from the receiver indicates the direction in the local tangent space which takes the predicted value closest in terms of $d[t]$ to the actual precoders. For prediction, we use a lifting map to obtain local tangent spaces, optimize linear functions in the local tangent spaces, and then use a retraction map that corresponds to the chosen lifting map to return to the manifold. The lifting map to obtain the tangent space and the retraction map to return to the manifold include the maps described in Section III, though several such maps exist. We obtain the tangent from box (i,t) to nearby box (j,s) as $\mathbf{T}^{j,s}_{i,t}$ from $\tilde{\mathbf{U}}_{i,t}$ to $\tilde{\mathbf{U}}_{j,s}$ using the chosen lifting operation, denoted by $\mathbf{T}^{j,s}_{i,t} = \mathtt{lift}_{\tilde{\mathbf{U}}_{i,t}}\left(\tilde{\mathbf{U}}_{j,s}\right)$. The corresponding retraction operation to map back to the manifold is given by $\mathtt{retract}_{\tilde{\mathbf{U}}_{i,t}}\left(\mathbf{T}^{j,s}_{i,t}\right)$.

$\mathbf{T}^{j,s}_{i,t}$ can be approximated by a linear combination of two matrices that represent the tangent matrices in time and frequency domain separately, local to (i,t). In other words, there exist matrices $\mathcal{T}_{i,t}, \mathcal{F}_{i,t}$ such that $\mathbf{T}^{j,s}_{i,t} \approx \mathcal{F}_{i,t}\Delta f + \mathcal{T}_{i,t}\Delta t$, where $\Delta f, \Delta t \in \mathbb{Z}$ are small steps in the time and frequency axes respectively. In our case, we choose $\Delta f = j - i$ and $\Delta t = s - t$, i.e. the signed frequency/time separation between boxes (j,t) and (i,t). We estimate $\mathcal{F}_{i,t}, \mathcal{T}_{i,t}$ using a least-squares fit over the known tangents to $(j,s) \in \mathtt{nbrs}_{i,t}(p)$. $\mathtt{nbrs}_{i,t}(p)$ (defined below)

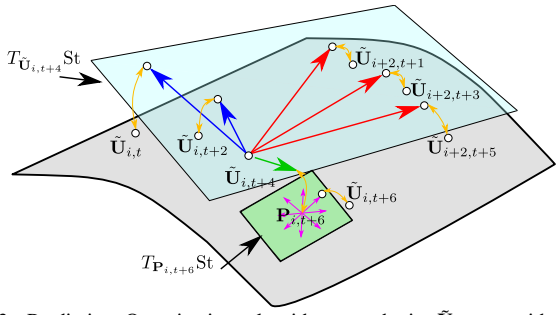

Fig. 3: Predictive Quantization algorithm to obtain $\tilde{\mathbf{U}}_{i,t+6}$, with closest previous value being $\tilde{\mathbf{U}}_{i,t+4}$. The yellow curves represent the lifting/retraction operations. $\mathbf{P}_{i,t+6}$ is the predicted value of $\tilde{\mathbf{U}}_{i,t+6}$. The blue and green planes are the tangent spaces local to $\tilde{\mathbf{U}}_{i,t+4}$ and $\mathbf{P}_{i,t+6}$ respectively. The local tangent space at $\mathbf{P}_{i,t+6}$ is then quantized and fed back to obtain $\tilde{\mathbf{U}}_{i,t+6}$.

refers to the collection of neighbours (j,s) of (i,t), which are lifted to the tangent space local to i,t for estimating $\mathcal{F}_{i,t}, \mathcal{T}_{i,t}$. Let $\texttt{same\_freq\_nbrs}_{i,t}(p) = \{(i, t-2m) | m \in \{1 \dots p-1\}\}$, $\texttt{diff\_freq\_nbrs}_{i,t}(p,q) = \{(i+q\delta_f, t-2m+1) | m \in \{1 \dots p\}\}$, where p is the number of past samples considered, $q = +1/-1$, indicating right/left neighbors. To ensure that $\mathbf{\Delta}_{i,t}$ is invertible, we take frequency separations only on one side.

$$\texttt{nbrs}_{i,t}(p) = \begin{cases} \texttt{same\_freq\_nbrs}_{i,t}(p) \bigcup \texttt{diff\_freq\_nbrs}_{i,t}(p,1), & \text{for } i \neq N-1 \\ \texttt{same\_freq\_nbrs}_{i,t}(p) \bigcup \texttt{diff\_freq\_nbrs}_{i,t}(p,-1), & \text{for } i = N-1 \end{cases} \quad (4)$$

where N is the total number of subcarriers, indexed from 0. In Fig. 2, the purple encircled boxes are $\texttt{nbrs}(\tilde{\mathbf{U}}_{i,t+4}(3))$ and $\texttt{nbrs}(\tilde{\mathbf{U}}_{i+8,t+4}(3))$ respectively.

$$\mathcal{F}_{i,t}, \mathcal{T}_{i,t} \leftarrow \text{argmin} \sum_{(j,s)\in \texttt{nbrs}_{i,t}(p)} ||(\mathcal{F}_{i,t}(j-i) + \mathcal{T}_{i,t}(s-t) - \mathbf{T}_{i,t}^{j,s})||_F^2 \quad (5)$$

where $||\cdot||_F$ represents Frobenius norm. We use the identities $\frac{\partial}{\partial X}(\text{Tr}(\mathbf{AXB})) = \mathbf{A}^H\mathbf{B}^H$ and $\frac{\partial}{\partial \mathbf{X}}\left(\text{Tr}(\mathbf{AX}^H\mathbf{B})\right) = \mathbf{BA}$, where $\mathbf{A}, \mathbf{X}, \mathbf{B}$ are matrices such that products $\mathbf{AXB}$ and $\mathbf{AX}^H\mathbf{B}$ exist. Taking partial derivatives of the objective function in (5) with respect to $\mathcal{F}_{i,t}, \mathcal{T}_{i,t}$ and setting them to be the null matrix gives,

$$\begin{bmatrix} \mathcal{F}_{i,t} \\ \mathcal{T}_{i,t} \end{bmatrix} = \mathbf{\Delta}_{i,t}^{-1} \begin{bmatrix} \Sigma_{j,s}(j-i)\mathbf{T}_{i,t}^{j,s} \\ \Sigma_{j,s}(s-t)\mathbf{T}_{i,t}^{j,s} \end{bmatrix} \quad (6)$$

$$\mathbf{\Delta}_{i,t} = \begin{bmatrix} \Sigma_{j,s}(j-i)^2 & \Sigma_{j,s}(j-i)(s-t) \\ \Sigma_{j,s}(j-i)(s-t) & \Sigma_{j,s}(s-t)^2 \end{bmatrix} \quad (7)$$

As an example, to predict the precoding matrix at box (k,l): When the temporal correlation of the channel is higher than the frequency correlation, $(i,t) = (k, l-2)$, and if the frequency correlation is larger, $(i,t) = (k \pm 2, l-1)$. The chosen (i,t) is likely to be closest among the past fed back points, in terms of chordal distance, to the new box (k,l). The chosen (i,t) is referred to as the center (anchor point) on whose local tangent space we optimize to obtain $\mathcal{F}_{i,t}, \mathcal{T}_{i,t}$ using the known neighbouring boxes (j,s) around the center (i,t). We thus obtain the predicted precoder at box (k,l) given by $\mathbf{P}_{k,l} = \text{retract}(\tilde{\mathbf{U}}_{i,t}, \mathcal{F}_{i,t}(k-i) + \mathcal{T}_{i,t}(l-t))$. $\mathbf{P}_{k,l}$ is the outcome of the predictive quantization algorithm for box (k,l). Note that these operations can be conducted at the transmitter independently without any additional feedback.

Once we obtain the prediction $\mathbf{P}_{k,l}$, the receiver quantizes the tangent space local to $\mathbf{P}_{k,l}$ using a $\mathcal{B}$ bit codebook and feeds back the optimal index, which the receiver uses to obtain $\tilde{\mathbf{U}}_{k,l}$. The approach to quantize the tangent space local to the prediction has been discussed in [8, 11]. We adopt the strategy in [11], which controls the spread of codewords by having two codebooks T_p^C, T_m^C of different spreads, but same $2^{\mathcal{B}-1}$ base vectors $\in T_{\mathbf{P}_{k,l}}\text{St}(N_T, N_R)$. These base vectors belong to a common base codebook $\mathcal{T}^B$. However, T_p^C covers more volume than T_m^C. The two codebooks are concatenated to form T^C, and the receiver feeds back the optimal index c_n, that minimizes the chordal distance to the actual value via (8). The transmitter uses (9) and fed back c_n to calculate $\tilde{\mathbf{U}}_{k,l}$.

$$c_n \leftarrow \text{argmin}_{i \in 2^{\mathcal{B}}} \left(d_s\left(\mathbf{U}_{k,l}, \text{retract}(\mathbf{P}_{k,l}, T^C[i])\right)\right) \quad (8)$$

$$\tilde{\mathbf{U}}_{k,l} = \text{retract}(\mathbf{P}_{k,l}, T^C[c_n]) \quad (9)$$

In [11], the base codebook, $\mathcal{T}^B$ was initialized randomly. However, we propose a VQ based initialization to guarantee isotropic base codewords, discussed further in Section V.

B. Joint Time-Frequency Interpolation scheme

Once the frequency-time bin matrix has been filled according to the hopping and predictive quantization scheme proposed in Section IV-A, the next step at the transmitter is to fill in the non fed back boxes (k,l). This is also done by estimating the $\mathcal{F}_{i,t}, \mathcal{T}_{i,t}$ at the closest fed back subcarrier (i,t) to subcarrier (k,l) by least-squares optimization. To interpolate we use future nearby feed back points, as shown in Fig. 4, since past fed back points' information has already been captured in the predictive quantization algorithm. Define,

$$\texttt{l\_nbrs}_{i,t}(p) = \texttt{same\_freq\_nbrs}_{i,t}(-p) \bigcup \texttt{diff\_freq\_nbrs}_{i,t}(-p,-1) \quad (10)$$

$$\texttt{r\_nbrs}_{i,t}(p) = \texttt{same\_freq\_nbrs}_{i,t}(-p) \bigcup \texttt{diff\_freq\_nbrs}_{i,t}(-p,1) \quad (11)$$

as the left/right neighbors at (i,t) (marked in dark/light green, purple for $(i+3, t+1)$ in Fig. 4). We obtain separate $\mathcal{F}_{i,t}$ for left (right) frequencies, viz. $\mathcal{F}_{i,t}^L$ ($\mathcal{F}_{i,t}^R$) from $\texttt{l\_nbrs}_{i,t}(p)$ ($\texttt{r\_nbrs}_{i,t}(p)$), to avoid singular $\mathbf{\Delta}_{i,t}$ when estimating $\mathcal{F}_{i,t}$.

$$\mathcal{F}_{i,t}^L, \mathcal{T}_{i,t}^L \leftarrow \text{argmin}\left(\textstyle\sum_{(j,s)\in \texttt{l\_nbrs}_{i,t}(p)} \left(||(\mathcal{F}_{i,t}(j-i) + \mathcal{T}_{i,t}(s-t) - \mathbf{T}_{i,t}^{j,s})||_F^2\right)\right) \quad (12)$$

$$\mathcal{F}_{i,t}^R, \mathcal{T}_{i,t}^R \leftarrow \text{argmin}\left(\textstyle\sum_{(j,s)\in \texttt{r\_nbrs}_{i,t}(p)} \left(||(\mathcal{F}_{i,t}(j-i) + \mathcal{T}_{i,t}(s-t) - \mathbf{T}_{i,t}^{j,s})||_F^2\right)\right) \quad (13)$$

The interpolated estimates for non-fed back boxes (k,l) are

$$\tilde{\mathbf{U}}_{k,l} = \begin{cases} \text{retract}(\tilde{\mathbf{U}}_{i,t}, \mathcal{F}_{i,t}^L(k-i) + \mathcal{T}_{i,t}^L(l-t)), & \text{for } k < i \\ \text{retract}(\tilde{\mathbf{U}}_{i,t}, \mathcal{F}_{i,t}^R(k-i) + \mathcal{T}_{i,t}^R(l-t)), & \text{for } k \geq i \end{cases} \quad (14)$$

The fed back boxes (i,t) obtained by predictive quantization act as centers to obtain the interpolated estimate of boxes $(k,l) \in \texttt{cluster}(i,t)$, which is defined as

$$\texttt{cluster}(i,t) = \begin{cases} \{(i-\delta_f+p, t+q) \ | p \in \{0,1,\dots 2\delta_f\}, q \in \{0,1\}\} \setminus (i,t), & \text{for } i \neq \{0, N-1\} \\ \{(i+p, t+q) \ | p \in \{0,1,\dots \delta_f\}, q \in \{0,1\}\} \setminus (i,t), & \text{for } i = 0 \\ \{(i-\delta_f+p, t+q) \ | p \in \{0,1,\dots \delta_f\}, q \in \{0,1\}\} \setminus (i,t), & \text{for } i = N-1 \end{cases} \quad (15)$$

For optimal power allocation via waterfilling, the singular values should also be fed back. We quantize these using vector quantization and feed them back at equally spaced indices (shown in Fig. 1). At the receiver, these are interpolated at the unknown subcarriers using linear interpolation (Predictive quantization is not performed for the singular values).

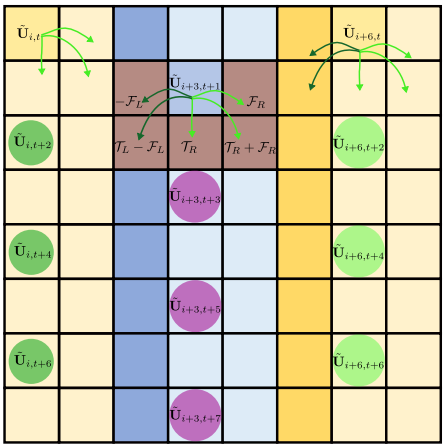

Fig. 4: Each fed back precoder (i,t) uses neighbor future information to estimate it's $\texttt{cluster}(i,t)$. The brown shaded cells form $\texttt{cluster}(i+3,t+1)$.

V. Simulation Results

We simulated our algorithms by using py-itpp python wrapper for IT++ [17]. Channels were generated using Jake's model with an ITU Vehicular-A profile for all the simulations, and $N_T = 4$ and $N_R = 2$, with 1024 subcarriers. The codes used to generate the results are available in a public repository [18].

A. Proposed Interpolation on $St(N_T, N_R)$

We consider an OFDM system with $N = 1024$ subcarriers. Keeping with the labeling in Fig. 2, we use $D_f = 33$, i.e. the receiver feeds back precoder for 32 equally spaced feedback points at indices $33k, k = 0, 1, 2 \ldots 31$. The transmitter interpolates over 4×2 $\tilde{\mathbf{U}}_{i,t}$ via (3) and over 4×4 $\tilde{\mathcal{U}}_{i,t}$ via (2).

1) Codebook Generation: A 6 bit codebook for both 4×2 and 4×4 matrices is constructed using the Lloyd codebook algorithm [9]. This is done by generating 10,000 such $\mathbf{U}_{i,t}$'s and $\mathcal{U}_{i,t}$'s. We, therefore, use $32\times 6 = 192$ bits per OFDM frame for precoder feedback for both the cases.

2) Results: The results in Fig. 5 were obtained by averaging over 100 simulations runs. We observe approximately 3 dB gain at 10^{-3} BER with QPSK (MMSE equalization) when comparing the Cayley Exp. map BER with the geodesic BER. Note that, when interpolation is done over the ideal unquantized precoders (i.e. over $\mathbf{U}_{i,t}$, $\mathcal{U}_{i,t}$, instead of $\tilde{\mathbf{U}}_{i,t}$, $\tilde{\mathcal{U}}_{i,t}$), we do not observe performance benefit.

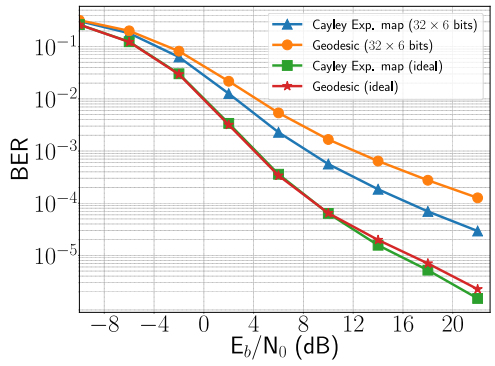

Fig. 5: BER results for comparing interpolation approaches.

This ascertains the fact that reduction in BER is achieved since we do not quantize redundant information when interpolating directly on $St(N_T, N_R)$. By dispensing with this redundant information, we can encode more information with lesser quantization error using the same number of bits.

B. Predictive Quantization and joint time-freq. interpolation

We now consider the hopping pattern of feedback indices (shown in Fig. 2), i.e. $\delta_f = 16$, with $D_f = 33$ and $N = 1024$. To compare this with the time based predictive quantization and frequency interpolation scheme as in Fig. 1, we feed back indices of the form $33k$. For interpolation in the time based approach (Fig. 1), we utilize the Cayley Exp. map. The simulations for the algorithm were done for a normalized Doppler $f_d T_s = 3.5\times 10^{-4}$, unless mentioned otherwise.

1) Codebook generation: Since both the time based and hopping based predictive quantization methods predict based on past fed back information, we initialize the system with the 6 bit Lloyd codebook for $\mathrm{St}(4,2)$ obtained in Section V-A1. Once sufficient past values of $\tilde{\mathbf{U}}_{i,t}$ have been quantized and fed back in advance, the algorithms can be used to start improving upon the quantization chordal error by exploiting the correlations available. An additional 2 bit k-means codebook was used to feed back quantized singular values for waterfilling.

To obtain the base codebook, $\mathcal{T}^B$, for $T_{\mathbf{P}_{k,l}}\mathrm{St}(N_T, N_R)$, we consider 10,000 independent channel evolutions. For each one, we use the evolution of the channel over 10 OFDM frames' duration to obtain a reliable prediction from both methods. We collect the vectors representing the skew Hermitian tangents ($\mathrm{lift}_{\mathbf{P}_{k,l}}(\mathbf{U}_{k,l})$, recall that Cayley Exp. map has skew Hermitian matrices as images (Section III)). This is done to get 10,000 independent predictions that give the same number of independent vectors in the collection. We then apply k-means algorithm to get a 6 bit codebook, $\mathcal{T}^B$, for $T_{\mathbf{P}_{k,l}}\mathrm{St}(N_T, N_R)$, for both the hopping based and time based schemes. Hence we transmit 32×6 bits per frame, which indicate the optimum tangent, which the transmitter can select to refine the estimated precoder predictions for appropriate fed back subcarriers.

2) Estimate chordal distance, $d[t]$ results: From Fig. 6 we observe that with time, $d[t]$ for the hopping predictive quantization scheme becomes much lower than that of the time based approach. We observed that after a certain time instant, the chordal distance on the Stiefel Manifold bumps up, which was observed even in [11]. Hence, we propose a scheme in which we reset the prediction algorithm and re-initialize with the 6 bit Lloyd codebook obtained for $\mathrm{St}(4,2)$ when such a situation is observed. Note that, even for initialization, we communicate 192 bits per frame only, which allows the algorithm to reset upon facing unpredictable heavy interference.

3) Results for hopping scenario: Fig. 7 shows BER performance (QPSK, MMSE equalization), averaged over 10 independent channel evolutions, and in each evolution, the algorithm was run till a sudden jump in quantization error was observed (as in [11]). Upon encountering the jump, we reset the algorithm using the independent 6 bit codebook.

By performing predictive quantization on our hopping strategy, and doing joint time-frequency interpolation, we have matched the *ideal* 32 subcarrier feedback BER performance, i.e. the case in which the transmitter is assumed to know the

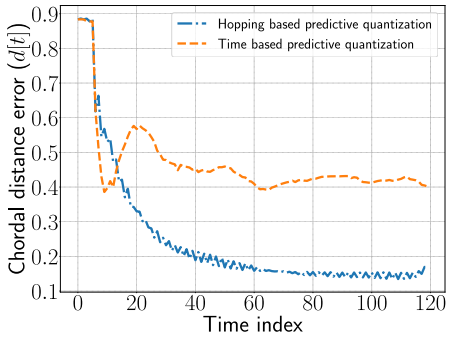

Fig. 6: Chordal distance error ($d[t]$) vs. time for one channel realization.

ideal unquantized precoding matrices for 32 equally spaced subcarriers in each OFDM frame and interpolates over frequency to find precoders at non fed back subcarriers, labeled "Cayley Exp. map (32, ideal)" in Fig. 7. The 63 subcarrier ideal feedback BER curve, labeled "Cayley Exp. map (63, ideal)", serves as a lower bound on the achievable BER performance for our hopping strategy. This scenario indicates that the transmitter has knowledge of ideal unquantized precoders at 32 equally spaced indices along with 31 middle indices of the regular intervals between them, in each OFDM frame, and performs interpolation as before. Hence, matching that curve would mean exploiting temporal and frequency correlations perfectly. We also observe a 2 dB gain at 10^{-4} BER when compared to the time based approach.

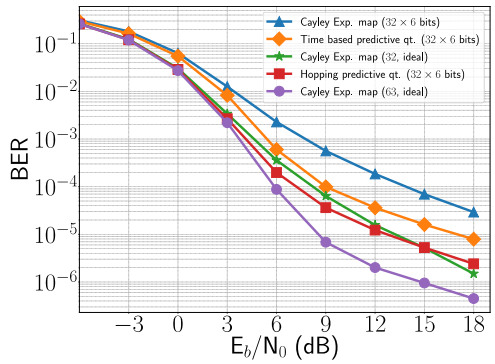

Fig. 7: BER vs E_b/N_0 for various interpolation strategies.

We obtain the achievable rates in Fig. 8 by averaging similarly, and the singular values are sent and interpolated like in Section V-A. When the channel varies faster, the time approach tracks the channel more efficiently due to higher temporal information. For slower channels, utilizing the frequency correlation is more valuable, since temporal variation is less significant, because of which the hopping approach outperforms the time approach. The crossover is at $f_d T_s = 10^{-2}$, which is generally a very fast varying channel.

VI. Conclusions

In this paper, we first proposed a new method of directly interpolating precoders on the Stiefel manifold and empirically showed that it offers a better performance than the traditional geodesic scheme. We then proposed a hopping strategy, coupled with a predictive quantization scheme and a joint time-frequency interpolation technique to utilize both the time

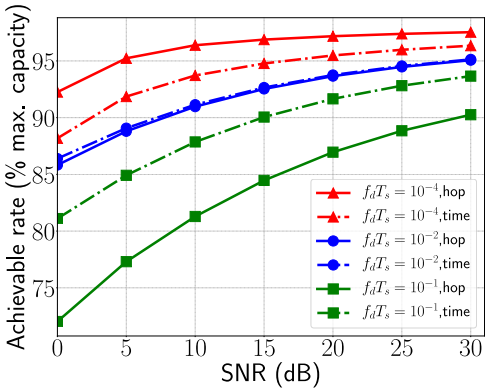

Fig. 8: Achievable rate of the prediction algorithm with SNR and $f_d T_s$.

and frequency correlations simultaneously. The proposed joint time-frequency scheme brings the BER and achievable rates close to that obtained using exact unquantized precoders. Future work involves study with various antenna configurations and the impact on performance with different channel profiles.

References

[1] D. J. Love, R. W. Heath, V. K. Lau, D. Gesbert, B. D. Rao, and M. Andrews, "An overview of limited feedback in wireless communication systems," *IEEE J. Sel. Areas Commun.*, vol. 26, no. 8, 2008.

[2] N. Khaled, B. Mondal, R. W. Heath, G. Leus, and F. Petré, "Quantized multi-mode precoding for spatial multiplexing MIMO-OFDM systems," in *IEEE 62nd Vehic. Technol. Conf.*, vol. 2. IEEE, 2005, pp. 867–871.

[3] R. T. Krishnamachari and M. K. Varanasi, "On the geometry and quantization of manifolds of positive semi-definite matrices," *IEEE Trans. Signal Process.*, vol. 61, no. 18, pp. 4587–4599, 2013.

[4] D. Sacristán-Murga and A. Pascual-Iserte, "Differential feedback of MIMO channel Gram matrices based on geodesic curves," *IEEE Trans. Wireless Commun.*, vol. 9, no. 12, pp. 3714–3727, 2010.

[5] T. Inoue and R. W. Heath, "Grassmannian predictive coding for limited feedback multiuser MIMO systems," in *ICASSP*, 2011, pp. 3076–3079.

[6] T. Li, F. Li, and C. Li, "Manifold-based predictive precoding for the time-varying channel using differential geometry," *Wireless Networks*, vol. 22, no. 8, pp. 2773–2783, Nov 2016.

[7] C.-B. Chae, D. Mazzarese, N. Jindal, and R. W. Heath, "Coordinated beamforming with limited feedback in the MIMO broadcast channel," *IEEE J. Sel. Areas Commun.*, vol. 26, no. 8, 2008.

[8] S. Schwarz, R. W. Heath, and M. Rupp, "Adaptive Quantization on a Grassmann-Manifold for Limited Feedback Beamforming Systems," *IEEE Trans. Signal Process.*, vol. 61, no. 18, pp. 4450–4462, Sept 2013.

[9] R. Pitaval and O. Tirkkonen, "Joint Grassmann-Stiefel Quantization for MIMO Product Codebooks," *IEEE Trans. Wireless Commun.*, vol. 13, no. 1, pp. 210–222, January 2014.

[10] R. Chakraborty and B. C. Vemuri, "Statistics on the (compact) Stiefel manifold: Theory and Applications," *CoRR*, vol. abs/1708.00045, 2017. [Online]. Available: http://arxiv.org/abs/1708.00045

[11] S. Schwarz and M. Rupp, "Predictive Quantization on Stiefel Manifold," *IEEE Signal Process. Lett.*, vol. 22, no. 2, pp. 234–238, Feb 2015.

[12] K. Schober, R. Pitaval, and R. Wichman, "Improved User-Specific Channel Estimation Using Geodesical Interpolation at the Transmitter," *IEEE Wireless Commun. Lett.*, vol. 4, no. 2, pp. 165–168, April 2015.

[13] Y. Chou and T. Sang, "Efficient interpolation of precoding matrices in MIMO-OFDM systems," in *SPAWC, 2010*, June 2010, pp. 1–4.

[14] Y. Li, S. Zhu, H. Tong, and M. Xu, "Enhanced limited rate implicit CSI feedback and its usage in covariance matrix based MU-MIMO," in *WCNC, 2013*. IEEE, 2013, pp. 3067–3071.

[15] Y. Jeon, H. Kim, Y. Cho, and G. Im, "Time-Domain Differential Feedback for Massive MISO-OFDM Systems in Correlated Channels," *IEEE Trans. Commun.*, vol. 64, no. 2, pp. 630–642, Feb 2016.

[16] K. A. Krakowski, L. Machado, F. S. Leite, and J. Batista, "A modified Casteljau algorithm to solve interpolation problems on Stiefel manifolds," *J. of Comp. and Appl. Math.*, vol. 311, pp. 84–99, 2017.

[17] V. Saxena, https://github.com/vidits-kth/py-itpp.

[18] https://github.com/Agrim9/Lim.-Feedback-MIMO-OFDM-Precoding.